

# A potentiometric and spectroscopic study of copper(II) diamidodiamino complexes †

Graham E. Jackson,\* Peter W. Linder and Alexander Voyé

Department of Chemistry, University of Cape Town, Rondebosch 7700, Cape Town, South Africa

Five diamidodiamino compounds, *N,N'*-bis[2-(dimethylamino)ethyl]propanediamide dihydrochloride  $L^2 \cdot 2HCl$ , *N,N'*-bis[2-(diethylamino)ethyl]propanediamide dihydrochloride ( $L^5$ ), *N,N'*-bis[2-(dimethylamino)ethyl]- and *N,N'*-bis[2-(diethylamino)ethyl]-ethanediamide ( $L^1$  and  $L^4$ ) and *N,N'*-bis[2-(dimethylamino)propyl]-ethanediamide ( $L^3$ ), have been synthesized and characterized. Their acid-base behaviour and complexation with copper(II) ions in aqueous solution at 25 °C and  $I = 0.15 \text{ mol dm}^{-3} \text{ Cl}^-$  have been investigated by potentiometric and spectrophotometric techniques. Relatively small differences observed between the protonation constants may be explained in terms of electronic induction effects of the alkyl side chains. The primary and tertiary amine groups show differences in basicity which conform to the general pattern of behaviour found with amines and attributable to changes in solvation of the reacting species in the protonation reactions. Copper(II) ions have been found to form several soluble complexes with  $L^1$ – $L^4$ . On the other hand,  $L^5$  precipitates in the presence of copper(II) ions. The stoichiometries of the mononuclear copper(II) complexes are proposed as  $CuL$ ,  $CuLH_{-1}$  and  $CuLH_{-2}$  with  $L^3$  also forming  $CuLH_{-3}$ . Dinuclear complexes,  $Cu_2LH_{-2}$  are proposed for  $L^1$ ,  $L^3$  and  $L^4$ . In addition,  $Cu_2LH_{-3}$  is proposed for  $L^1$ . The co-ordination sites and structures are suggested to be as follows:  $CuL$ , two contiguous chelate rings with the copper(II) co-ordinated to one amine N, one amide N and one carboxylate O;  $CuLH_{-1}$ , similar to  $CuL$  but with co-ordination to both amide N and one of the amine N;  $CuLH_{-2}$ , three contiguous chelate rings with co-ordination to all four N;  $CuLH_{-3}$ , the same as  $CuLH_{-2}$  but with a proton removed from a water molecule axially co-ordinated to the copper;  $Cu_2LH_{-2}$  ( $L = L^1$  or  $L^4$ ) and  $Cu_2LH_{-3}$  ( $L = L^1$ ), similar to  $CuL$  but incorporating two sets of co-ordination sites, one amine N plus one amide N plus one carboxylate O, per copper, giving four contiguous chelate rings; in  $Cu_2LH_{-3}$  a proton is removed from a water molecule co-ordinated to one of the coppers;  $Cu_2LH_{-2}$  ( $L = L^3$ ), one of the coppers is co-ordinated to all four N and the other to the two carboxylate O.

Earlier papers<sup>1</sup> in this series have been concerned with compounds that possess the potential of facilitating transport of copper in human blood plasma to sites of inflammation that occur in cases of rheumatoid arthritis. The approach has been two-fold, the first step involving evaluation of a given compound in respect of its ability to mobilize copper in human plasma. This evaluation is carried out by calculating the plasma mobilization index (p.m.i.) using the ECCLES<sup>2</sup> metal speciation program in conjunction with the most up-to-date thermodynamic database of metal-low-molecular-mass (l.m.m.) ligand equilibria applicable to human blood plasma.<sup>1</sup> Stability constants of complexes formed between the therapeutic compound, under investigation, and each of the metals occurring in human blood plasma need to be added to the thermodynamic database. The second step in investigating the potentially anti-inflammatory compound has been to seek confirmation of the ECCLES predictions through animal experiments<sup>3</sup> in which the effect of the candidate on the biodistribution of copper is investigated.

The ECCLES results indicate promise for 3,6,9,12-tetraaza-tetradecanedioate (ttda) and 3,6,9-triazaundecanedioate (dtda) as vehicles for delivery of copper to sites of inflammation.<sup>1</sup> The complementary animal experiments to be published elsewhere showed these compounds to be not biologically active, however, in that their copper complexes are rapidly excreted intact in the urine. This discrepancy may be explained as follows. Although the predominant copper complex in each case, under physiological conditions, is formally electrically neutral, these species are actually zwitterionic with the carboxylate groups

uncomplexed and negatively charged. The attendant hydrophilicity of these complexes favours renal filtration rather than transport across lipophilic membranes to body organs or sites of inflammation.

The foregoing conclusion prompts specification of an additional requirement to those itemized in ref. 1, for a successful copper-transporting compound in human blood plasma, namely that hydrophilicity should be reduced by ensuring embedment of ionic charges within the complex. With the total set of requirements in mind, the compounds described in this paper have been designed. Here, we describe their synthesis together with a study of the aqueous equilibria with hydrogen and copper(II) ions. The results elucidate the stoichiometry and solution structures of the complexes as well as providing the necessary stability constants as input to ECCLES. The ECCLES speciation and the biodistribution results will be published elsewhere.

## Experimental

### Reagents and solutions

All solutions were prepared from Merck Guaranteed Reagents or BDH Aristar grade chemicals using glass-distilled deionized water which had been boiled out in order to remove dissolved carbon dioxide. The copper(II) solutions were prepared from the dihydrated chloride salt and standardized against ethylenedinitrilotetraacetate (edta) solution using Fast Sulphon Black F as indicator.<sup>4</sup> Hydrochloric acid and sodium hydroxide solutions were made up from Merck Titrisol ampoules and standardized potentiometrically against recrystallized borax

† Copper anti-inflammatory drugs in rheumatoid arthritis. Part 5.<sup>1</sup>

**Table 1** Summary of experimental and computational details

Potentiometer	Metrohm Titroprocessor E636
Electrodes	Metrohm EA109 glass, EA404 calomel reference
Calibration	Strong acid–strong base, ligand titrations: data processed by CALIBT (MAGEC) <sup>7</sup> and ESTA <sup>8</sup>
Burette	Metrohm Dosimat E635 fitted with a non-return valve to prevent back diffusion and controlled by the Metrohm Titroprocessor E636
$I/\text{mol dm}^{-3}$ , electrolyte	0.15, NaCl
$T/^\circ\text{C}$	25
Inert atmosphere	Commercial dinitrogen passed successively through 50% (w/w) KOH, Fieser's solution <sup>9</sup> and thermostatted background electrolyte
Calculation method	ESTA <sup>8</sup> with weighting; initial volume 0.05 cm <sup>3</sup> , emf 0.10 mV, titre volume 0.005 cm <sup>3</sup> ; with Debye–Hückel correction; output checked against MINQUAD <sup>10</sup>
UV/VIS	Philips Scientific SP1700, readings taken at 10 nm intervals. Solutions circulated through the titration vessel and a quartz flow-through cuvette thermostatted at 25 °C
Spectral analysis	Local BASIC program which uses Gaussian elimination with potential row pivoting to solve the extended Beer–Lambert law equation
NMR spectrometer	Varian VXR 200

(sodium tetraborate) and potassium hydrogenphthalate, respectively. The NaOH solutions were prepared under an atmosphere of nitrogen and stored in high-density Polythene bottles fitted with carbon dioxide (soda lime) traps. These solutions were used within 1 week or discarded. All solutions were made up to an ionic strength of 0.15 mol dm<sup>-3</sup> with respect to chloride using Aristar NaCl. Volumetric flasks were calibrated with deionized water allowing for the Archimedes effect on standard weights, the volumetric expansion of glass, and density changes at the water temperature.<sup>5</sup> The purity of all the pro-ligands used was checked by potentiometric titration and found to be >99%.

### Syntheses

***N,N'*-Bis[2-(dimethylamino)ethyl]propanediamide dihydrochloride (L<sup>2</sup>·2HCl).** Diethyl malonate (3.21 g, 0.020 mol) was slowly added to *N,N*-dimethylethane-1,2-diamine (3.78 g, 0.043 mol) and stirred under high-purity nitrogen for 3 h at 80 °C. The volume of the dark pink reaction mixture was reduced on a rotary evaporator. On standing, white radiating crystals in a hard pink matrix formed almost immediately. These were taken up in dry tetrahydrofuran (thf), the solution titrated with hexane and left to stand overnight, resulting in the formation of conglomerate, needle-shaped crystals. The very hygroscopic product was converted into the hydrochloride salt by dissolving the crystals in dry thf and bubbling dry HCl gas slowly through the solution. A hard white precipitate formed which was filtered off under nitrogen and recrystallized from a hot mixture of dry methanol and absolute ethanol titrated with thf. The large opaque crystals thus formed were washed with absolute ethanol followed by thf, dried under high vacuum and stored over P<sub>2</sub>O<sub>5</sub> (Found: C, 41.6; H, 8.0; N, 17.6. C<sub>11</sub>H<sub>24</sub>N<sub>4</sub>O<sub>2</sub>·2HCl requires C, 41.6; H, 8.2; N, 17.7%);  $\delta_{\text{H}}$ [200 MHz, solvent D<sub>2</sub>O, sodium 4,4-dimethyl-4-silapentane-1-sulfonate (dss)] 2.72 (12 H, s, CH<sub>3</sub>), 3.11 (4 H, t, *J* 6.0 Hz, MeNCH<sub>2</sub>), 3.17 (2 H, s, COCH<sub>2</sub>CO) and 3.42 (4 H, t, CONHCH<sub>2</sub>). The central methylene protons were observed to undergo slow deuterium exchange with the solvent.

***N,N'*-Bis[2-(diethylamino)ethyl]propanediamide dihydrochloride (L<sup>5</sup>·2HCl).** Diethyl malonate (3.2 g, 0.02 mol) was added to

*N,N*-diethylethane-1,2-diamine (5.1 g, 0.044 mol) and stirred under nitrogen for about 40 h at 70–80 °C. After the volume of the pink reaction mixture had been reduced on a rotary evaporator the product was isolated as a viscous oil. The oil was taken up in dry thf and HCl gas allowed to bubble slowly through the solution. A sticky, pale yellow precipitate was formed with the evolution of much heat. Recrystallization from dry MeCN, titrated with thf, resulted in a chunky white precipitate. This was filtered off under nitrogen, washed with thf and dried under high vacuum over P<sub>2</sub>O<sub>5</sub>. Yield 81% (Found: C, 48.0; H, 9.0; N, 15.1. C<sub>15</sub>H<sub>32</sub>N<sub>4</sub>O<sub>2</sub>·2HCl requires C, 48.3; H, 9.1; N, 15.0%);  $\delta_{\text{H}}$ (200 MHz, solvent CDCl<sub>3</sub>, standard SiMe<sub>4</sub>) 0.95 (12 H, t, *J* 7.1 Hz, CH<sub>3</sub>), 2.43 (12 H, t + q, MeCH<sub>2</sub>NCH<sub>2</sub>), 3.09 (2 H, s, COCH<sub>2</sub>CO) and 3.24 (4 H, d of t, CONHCH<sub>2</sub>);  $\delta_{\text{C}}$ (50 MHz, solvent CHCl<sub>3</sub>, standard SiMe<sub>4</sub>) 11.6 (CH<sub>3</sub>), 37.2 (CH<sub>2</sub>), 43.3 (COCH<sub>2</sub>CO), 46.7 (MeCH<sub>2</sub>), 51.2 (CH<sub>2</sub>) and 161.7 (CO). The central methylene protons underwent rapid deuterium exchange in D<sub>2</sub>O solution.

***N,N'*-Bis[2-(dimethylamino)ethyl]- and *N,N'*-bis[2-(diethylamino)ethyl]-ethanediamide (L<sup>1</sup> and L<sup>4</sup>).** The hydrochloride derivatives of these two compounds were synthesized as described previously<sup>6</sup> (Found: C, 39.4; H, 7.7; N, 18.5. C<sub>10</sub>H<sub>22</sub>N<sub>4</sub>O<sub>2</sub>·2HCl requires C, 39.6; H, 7.9; N, 18.5. Found: C, 47.0; H, 9.0; N, 15.6. C<sub>14</sub>H<sub>30</sub>N<sub>4</sub>O<sub>2</sub>·2HCl requires C, 46.8; H, 9.0; N, 15.6%).

***N,N'*-Bis[2-(dimethylamino)propyl]ethanediamide (L<sup>3</sup>).** *N,N*-Dimethylpropane-1,3-diamine (4.2 g, 0.041 mol) was added dropwise to diethyl oxalate (2.9 g, 0.02 mol) in dry thf (15 cm<sup>3</sup>) with the evolution of heat. The solution was stirred and allowed to reflux under nitrogen for about 24 h at 65 °C. The volume of the pale yellow solution was reduced to dryness on a rotary evaporator. The white precipitate was recrystallized from cold hexane. Yield 90% (Found: C, 55.2; H, 10.4; N, 21.7. C<sub>12</sub>H<sub>26</sub>N<sub>4</sub>O<sub>2</sub> requires C, 55.8; H, 10.1; N, 21.7%);  $\delta_{\text{H}}$ (200 MHz, solvent dss) 1.69 (4 H, t of t, CH<sub>2</sub>CH<sub>2</sub>CH<sub>2</sub>), 2.14 (12 H, s, CH<sub>3</sub>), 2.32 (4 H, distorted t, MeNCH<sub>2</sub>) and 3.25 (4 H, t, *J* 7.0 Hz, CONHCH<sub>2</sub>).

### Potentiometric studies

Protonation constants of the pro-ligands and stability constants of the copper(II) complexes were determined under the conditions given in Table 1. The concentrations of pro-ligands and of copper(II) covered the ranges given in the tables of results. The pH ranges covered are also given in these tables. Acidified solutions of pro-ligand were titrated with NaOH to high pH and then titrated with HCl back towards the initial pH. These titrations served to check the reversibility and reproductibility of each system, as well as to obtain protonation constants and electrode parameter values. To determine metal complex stability constants, acidified pro-ligand solution was titrated with NaOH to a high pH, copper(II) was added to the titration vessel and the resulting solution titrated in both directions, first with HCl and then with NaOH; the preliminary pro-ligand titration provided data for *in situ* calibration of the electrodes.

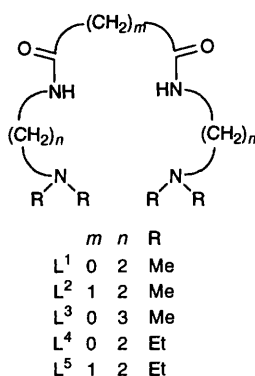
### Spectrophotometric studies

The copper binding sites in each of the complexes identified in the potentiometric studies were determined spectrophotometrically as outlined in Table 1. The electronic spectra also afforded elucidation of the solution structures of the complexes. Titrations similar to those in the potentiometric studies were carried out using similar concentration ranges of pro-ligand and copper(II) and covering similar pH ranges. The data consisted of sets of values of titre volume, electromotive force (emf) and absorbance (over a range of wavelengths).

**Table 2** Logarithms of protonation constants.  $n_T$  = Number of titrations,  $n_p$  = number of titration points,  $R^H$  = the Hamilton  $R$  factor;  $R_{lim}$  the lowest statistically significant  $R^H$ ,  $K_{H1}$  refers to the reaction  $L + H \rightleftharpoons HL$ ,  $K_{H2}$  to  $HL + H \rightleftharpoons H_2L$  (charges omitted for clarity);  $I$  = ionic strength

Compound	$n_T$	$n_p$	$c_L/\text{mmol dm}^{-3}$	pH Range	$R^H$ ( $R_{lim}$ )	$\log K_{H1}^*$	$\log K_{H2}^*$	$I/\text{mol dm}^{-3}$ , electrolyte ( $T/^\circ\text{C}$ )	Ref.
$L^1$	5	276	5.6–12.4	5.9–10.4	0.005 67 (0.004 23)	8.72 (0.002) 8.93	7.92 (0.002) 8.19	0.15, NaCl (25) 0.5, $\text{KNO}_3$ (25)	This work 13
$L^4$	3	229	10.3–19.1	6.0–11.1	0.001 99 (0.001 89)	9.23 (0.001)	8.49 (0.001)	0.15, NaCl (25)	This work
$L^{1'}$						9.31	8.43	0.10, $\text{KNO}_3$ (22)	14
$L^2$	17	822	9.0–17.6	5.2–11.6	0.005 34 (0.002 75)	8.83 (0.001)	8.07 (0.001)	0.15, NaCl (25)	This work
$L^5$	5	294	3.2–7.9	6.1–11.4	0.011 27 (0.006 90)	9.51 (0.002)	8.64 (0.003)	0.15, NaCl (25)	This work
$L^{2'}$						9.40	8.68	0.10, $\text{KNO}_3$ (22)	14
$L^3$	7	295	11.1–16.0	5.7–11.4	0.007 85 (0.001 32)	9.52 (0.002)	8.86 (0.002)	0.15, NaCl (25)	This work
$L^{3'}$						10.15	9.39	0.1 (25)	15

\* Standard deviation in parentheses.  $L^{1'}$ ,  $L^{2'}$ ,  $L^{3'}$  refer to  $L^1$ ,  $L^2$ ,  $L^3$  respectively where  $R = H$ .



that of the corresponding shorter one in  $L^2$ . On the other hand, the longer central alkyl chain of  $L^2$  has little inductive effect. Further, the basicities of the tetraethyl compounds are greater than those of their tetramethyl analogues, in conformity with ethyl having a greater inductive effect than methyl.

Considering the compounds  $L^1$  and  $L^{1'}$ ,  $L^2$  and  $L^{2'}$  and  $L^3$  and  $L^{3'}$ , in pairs, Table 2 shows the primary amines to be more basic than the respective tertiary amines. This conforms to the well known pattern of behaviour of amines<sup>16</sup> in which the order of basicity in aqueous solution is opposite to that in the gas phase. The gas-phase pattern is consistent with the prediction based on induction effects. On the other hand, the basicity order in aqueous solution is usually attributed to the change in solvation accompanying the conversion of the reactants into products.<sup>16,17</sup>

## Results and Discussion

### Ionic product of water

A value for  $pK_w$  of 13.73 was obtained from several strong acid–strong base titrations at  $I = 0.15 \text{ mol dm}^{-3}$ . Protonation titrations of potassium hydrogenphthalate yielded the same result. The value is in good agreement with those of Dyrssen and Hanson<sup>11</sup> (13.75 at  $I = 0.4 \text{ mol dm}^{-3}$ ) and Teder<sup>12</sup> (13.72 at  $I = 0.1 \text{ mol dm}^{-3}$ ).

### Protonations

Titrations were carried out with pro-ligand concentrations covering the ranges indicated in Table 2. The protonation curves ( $\bar{Z}_H$  vs.  $-\log[H^+]$ ) obtained for each pro-ligand showed sigmoidal shapes with limiting  $\bar{Z}_H$  values approaching 2.0. In Table 2 are also presented logarithms of the stepwise protonation constants obtained by ESTA<sup>8</sup> optimization together with literature values for  $L^1$  and for three other related pro-ligands. The agreement between our protonation constants for  $L^1$  and those reported by Zuberbühler and Kaden<sup>13</sup> is satisfactory, taking into account the different background media used. Our results show that, for the set of three tetramethyl compounds, the basicity of both Lewis-acid sites increases in the order  $L^1 < L^2 < L^3$ , the difference between  $L^1$  and  $L^2$  being slight whereas there are marked differences between these two, on the one hand and  $L^3$  on the other. These observations may be explained in terms of electronic induction. The inductive effect of the longer alkyl side chain in  $L^3$  exceeds

### Complexations

Of the five pro-ligands investigated in this study,  $L^5$  was found to not complex copper(II) effectively, resulting in precipitation throughout the titration. These results were therefore discarded. The other four were well behaved, giving rise to dissolved complexes of different stability and colour.

A problem that occurs commonly in the computational analysis of potentiometric data arises when two or more models describe the experimental data equally well as far as the statistical criteria are concerned. This problem was found to occur with the copper(II)– $L^1$  system. Three models were considered, comprising the sets of species  $ML$ ,  $MLH_{-1}$ ,  $MLH_{-2}$  and  $M_2LH_{-2}$ , plus either  $M_2LH_{-3}$  or  $M_2LH_{-4}$  or both of these. Since it was very difficult to decide between the first two models, constants for both have been presented in Table 3. Attempts to refine constants for species with more than one ligand per metal ion were unsuccessful. Model 1 has a reasonably low  $R$  factor and small standard deviations in  $\log \beta_{pqr}$  as well as a very good qualitative correspondence between calculated and observed plots for both  $\bar{Z}$  and  $\bar{Q}$  [Fig. 1(a) and 1(b)].<sup>1</sup> The formation curves, particularly those with higher ligand to metal ratios, level off at a value of  $\bar{Z}$  equal to 1, indicating the presence of  $ML$  as a major species. Thereafter the curves fan back indicating loss of amide protons upon metal-ion co-ordination.<sup>13,18,19</sup> Fig. 1 also shows that the formation curves corresponding to different ligand to metal concentration ratios are not superimposable indicating the presence of oligonuclear species. The  $\bar{Q}$  deprotonation curves for the

**Table 3** Logarithms of overall stability constants,  $\beta_{pqr}$ , of copper(II)-L<sup>-1</sup> complexes at 25 °C. Range of total ligand concentration = 4.7–10.7 mmol dm<sup>-3</sup>, range of total metal concentration = 2.45–7.5 mmol dm<sup>-3</sup>; pH range = 4.5–10.9 (this work);  $\beta_{pqr}$  refers to the reaction  $p\text{Cu} + q\text{L} + r\text{H} \rightleftharpoons \text{Cu}_p\text{L}_q\text{H}_r$  (charges omitted for clarity)

$n_T$	$n_p$	$R^H (R_{\text{lim}})$	Species			$\log \beta_{pqr}^*$	$I/\text{mol dm}^{-3}$ , electrolyte	Ref.
			$p$	$q$	$r$			
Model 1 8	588	0.010 88 (0.005 54)	1	1	0	8.33 (0.02)	0.15, NaCl	This work
			1	1	-1	1.06 (0.02)		
			1	1	-2	-7.06 (0.01)		
			2	1	-2	0.79 (0.01)		
			2	1	-3	-6.89 (0.03)		
Model 2 7	475	0.008 98 (0.005 42)	1	1	0	8.44 (0.01)	0.15, NaCl	This work
			1	1	-1	1.28 (0.01)		
			1	1	-2	-7.24 (0.01)		
			2	1	-2	0.74 (0.01)		
			2	1	-4	-15.36 (0.02)		
Literature			1	1	0	8.26	0.5, KNO <sub>3</sub>	13
			1	1	-1	0.55		
			1	1	-2	-7.44		
			2	1	-2	1.49		
			2	1	-3	-7.30		
			2	1	-4	-16.66		

\* Standard deviation in parentheses.

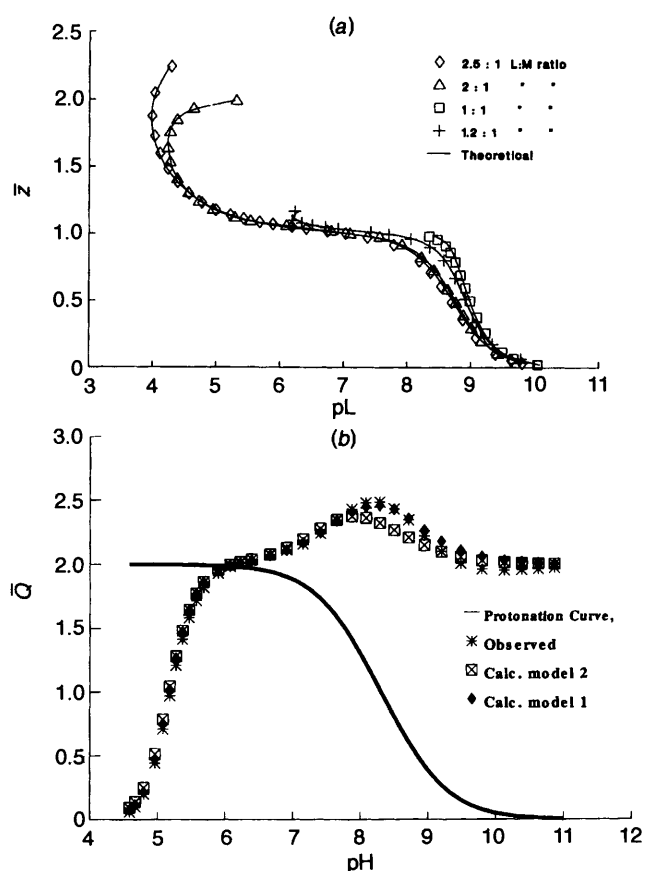


**Fig. 1** Plots of (a)  $\bar{Z}$ , the average number of ligands bound per metal ion, and (b)  $\bar{Q}$ , the average number of protons released from the ligand due to complexation for the system  $\text{Cu}^{\text{II}}\text{-L}^1$

copper(II)-L<sup>-1</sup> system were similar, so the observed and calculated plots of only one titration are shown in Fig. 1(b). The solid line in the figure represents the average number of protons bound to the ligand. This is an indication of the number of protons available, at a particular pH, for displacement by the metal ion. As can be seen the deprotonation function  $\bar{Q}$  rapidly moves up to intersect the protonation curve  $\bar{Z}_H$  at a pH of 6, reaching a maximum value of about 2.5 at pH 8.2. From here

on the  $\bar{Q}$  curves run roughly parallel to the protonation curve and then level off at a value of 2 in the strongly alkaline region. This means that from a pH of  $\approx 8.2$  onwards two additional protons have been displaced per metal ion from the ligand, resulting in the ligand losing a total of four protons. Since  $\bar{Q}$  is defined as the number of protons displaced per metal ion this could indicate the presence of a major species with a 1:2 metal to ligand stoichiometric ratio or a major 1:1 metal to ligand species with the displacement of two additional protons from the ligand. The second model in Table 3 had a slightly lower  $R$  factor, although based on the Hamilton test this is not significantly different from the first model. It also had smaller standard deviations in  $\log \beta_{pqr}$ . However this model shows a marked discrepancy between the observed and calculated  $\bar{Q}$  curves at high pH [Fig. 1(b)]. Thus, for the purposes of further calculations, model 1 was chosen as providing the best description of the copper(II)-L<sup>-1</sup> system. A third model which included both complexes was used by Zuberbühler and Kaden,<sup>13</sup> but in our work this model gave a high  $R$  factor, as well as large standard deviations in  $\log \beta_{pqr}$ . Furthermore a discrepancy between the observed and calculated  $\bar{Q}$  was observed as was the case for model 2. Since this model would have been expected to have shown the best statistical fit, as one additional parameter was being optimized, model 3 was disregarded. Fig. 2(a) gives the species distribution for a 2:1 ligand:metal ratio. From this it is seen that all five complexes are important, in particular the  $\text{MLH}_{-2}$  species in the basic region, and the  $\text{M}_2\text{LH}_{-2}$  binuclear complex between pH 5 and 7.5. At the same time, during the titration, the solution changes from an intense violet, through dark blue to a pale blue. (As described below, these colour changes were analysed spectrophotometrically to indicate the structure of the various species.)

The results for the copper(II)-L<sup>-4</sup> system are shown in Table 4. In contrast to the copper(II)-L<sup>-1</sup> system, only a slight splitting of the formation curves for different ligand to metal titration ratios is observed, indicating the oligonuclear species are of less importance for this system. This is also reflected in both the lower stability of the  $\text{M}_2\text{LH}_{-2}$  species and in the species distribution plot given in Fig. 2(b), where the curve for the  $\text{M}_2\text{LH}_{-2}$  species lies below that of the  $\text{ML}$  complex. The experimental solutions were also less intensely coloured throughout the titrations with a lighter shade of violet in the strongly alkaline region than in the case of the copper(II)-L<sup>-1</sup> system.

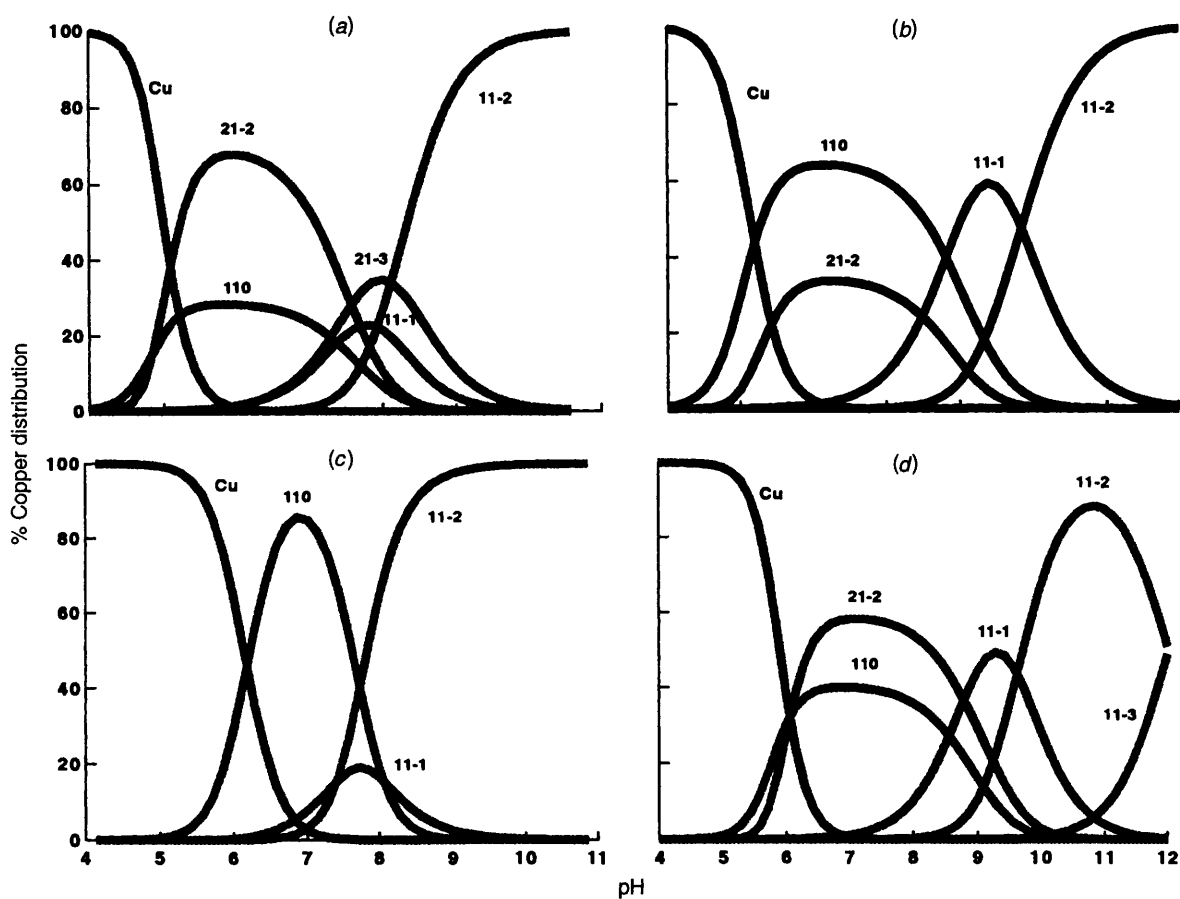


Fig. 2 Speciation diagrams for the systems (a)  $\text{Cu}^{\text{II}}\text{-L}^1$ , 2:1 ligand:metal ratio, (b)  $\text{Cu}^{\text{II}}\text{-L}^4$ , 2:1 ligand:metal ratio, (c)  $\text{Cu}^{\text{II}}\text{-L}^2$ , 4:1 ligand:metal ratio and (d)  $\text{Cu}^{\text{II}}\text{-L}^3$ , 2:1 ligand:metal ratio

Table 4 Logarithms of overall stability constants,  $\beta_{\text{pqr}}$ , of copper(II)-complexes with  $\text{L}^2\text{-L}^4$  at 25 °C and  $I = 0.15 \text{ mol dm}^{-3}$  (Na)Cl

Ligand	$n_{\text{T}}$	$n_{\text{p}}$	$c/\text{mmol dm}^{-3}$	pH Range	$R^{\text{H}}$ ( $R_{\text{lim}}$ )	Species			$\log \beta_{\text{pqr}}^*$
						$p$	$q$	$r$	
$\text{L}^4$	8	552	$c_{\text{L}}$ 5.2–17.9 $c_{\text{M}}$ 2.0–5.0	4.8–11.0	0.008 91 (0.004 11)	1	1	0	8.16 (0.01)
						1	1	-1	0.35 (0.005)
						1	1	-2	-8.49 (0.01)
						2	1	-2	-1.72 (0.03)
$\text{L}^2$	12	817	$c_{\text{L}}$ 8.0–19.1 $c_{\text{M}}$ 1.7–3.6	6.4–11.0	0.007 90 (0.005 36)	1	1	0	6.51 (0.01)
						1	1	-1	-1.54 (0.005)
						1	1	-2	-8.94 (0.002)
						1	1	0	8.39 (0.01)
$\text{L}^3$	7	524	$c_{\text{L}}$ 4.7–14.7 $c_{\text{M}}$ 1.7–3.8	5.0–11.5	0.005 91 (0.003 78)	1	1	-1	-0.17 (0.005)
						1	1	-2	-9.80 (0.005)
						1	1	-3	-21.87 (0.01)
						2	1	-2	-1.23 (0.02)
						1	1	-1	-0.17 (0.005)
						1	1	-2	-9.80 (0.005)

\* Standard deviation in parentheses.

In order to complete the homologous series, titrations with the compound  $\text{L}^3$  were carried out for various ligand to metal ratios from 2.7:1 to 4:1. In contrast to the other three systems the model best describing this system included the  $\text{MLH}_{-3}$  species. This species has been reported by Ojima and Nonoyama<sup>18</sup> for the compound  $\text{L}^1$ . The speciation diagram for the copper(II)- $\text{L}^3$  system [Fig. 2(d)] shows that the  $\text{MLH}_{-3}$  species becomes increasingly important accounting for about 25% of bound copper at a pH of 11.5. Apart from this additional species and the absence of the  $\text{M}_2\text{LH}_{-3}$  species, the speciation diagram is again quite similar to that of the copper(II)- $\text{L}^1$  system, although the curves have been shifted to higher pH values. Even so this compound is better able to solubilize copper(II) than is  $\text{L}^2$ , as is evident from a comparison of the positions of the copper aqua ion curves in the two speciation diagrams, presented in Fig. 2(c) and 2(d). This is

probably due to the stronger ML complex and the existence of the  $\text{M}_2\text{LH}_{-2}$  species in the case of  $\text{L}^3$ . The colour of the experimental solutions again changed during the course of the titrations but these changes were far less intense than observed for any of the other three systems.

#### Co-ordination sites and solution structures

Electronic spectra obtained for the individual species are shown in Fig. 3. The  $\lambda_{\text{max}}$  values of Fig. 3(a) agree reasonably well with the respective values published for copper(II)- $\text{L}^1$  complexes by Zuberbühler and Kaden.<sup>13</sup> In each case a single absorption band is seen which can be assigned to the spin-allowed Laporte-forbidden d-d transition,  ${}^2\text{E}_g \rightarrow {}^2\text{T}_{2g}$ . Since this is a  $d^9$  system, the crystal-field splitting is in turn affected by the co-ordination sphere of the metal ion and, hence,  $\lambda_{\text{max}}$  affords a measure of the

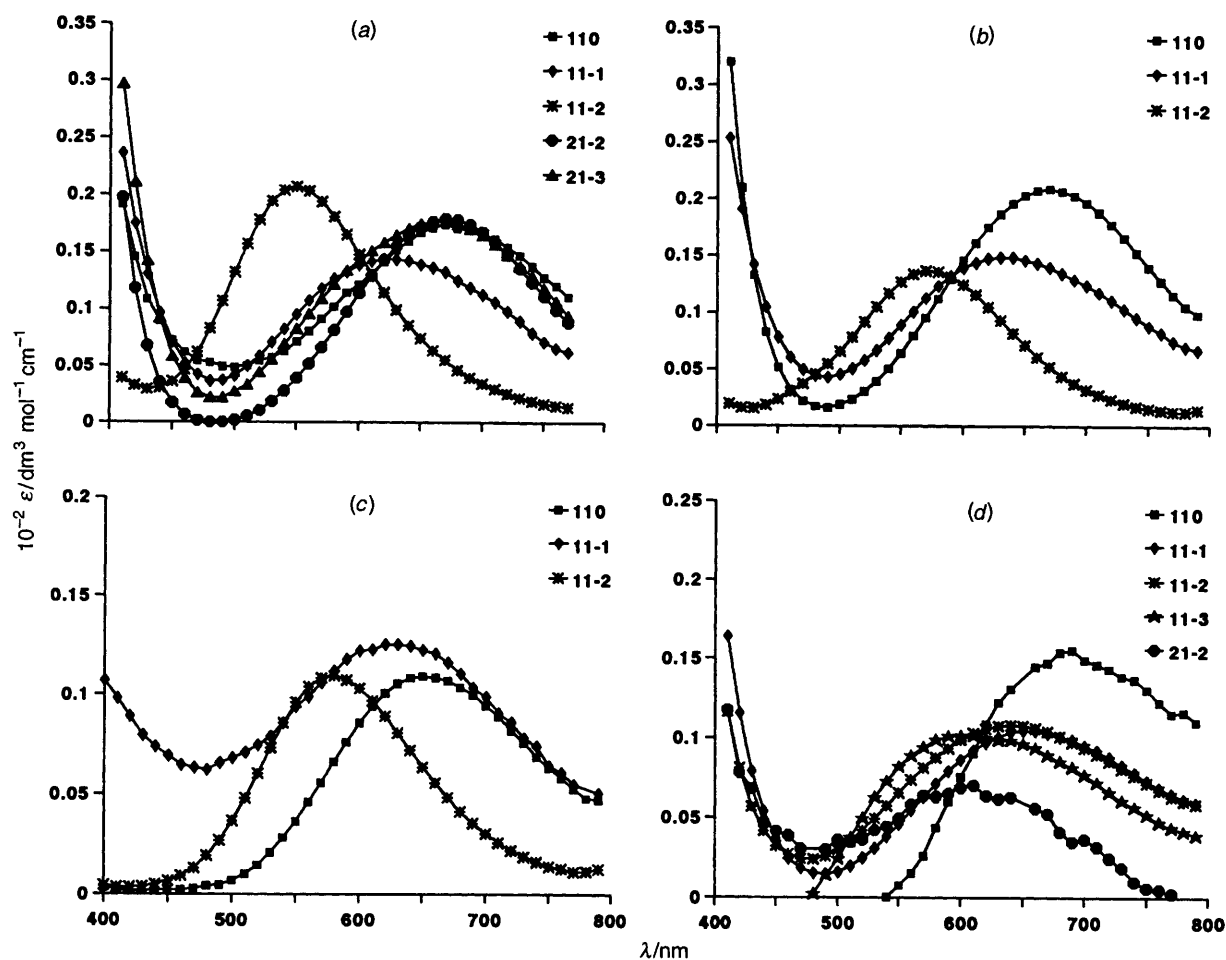


Fig. 3 Calculated electronic spectra of individual copper(II) complexes of (a)  $L^1$ , (b)  $L^4$ , (c)  $L^2$  and (d)  $L^3$

Table 5 Wavelengths in nm corresponding to the maximum absorption coefficients of the various copper(II) species formed in solution with compounds  $L^1$ – $L^4$ . For comparison literature values for  $L^1$  and  $L^6$  (refs. 13, 21) as well as for the  $[\text{Cu}(\text{NH}_3)_n(\text{H}_2\text{O})_{6-n}]^{2+}$  species<sup>20</sup> where  $n = 0$ –4 are also given

Ligand	<i>pqr</i>					
	1 1 0	1 1 – 1	1 1 – 2	2 1 – 2	2 1 – 3	1 1 – 3
$L^1$	675	620	550	670	665	—
$L^4$	670	630	570	*	—	—
$L^2$	650	625	575	—	—	—
$L^3$	690	660	640	600	—	610
$L^1$	650	630	550	660	670	—
$L^6$	690	670	(570)	680	590	—
$\text{NH}_3$ in $[\text{Cu}(\text{NH}_3)_n(\text{H}_2\text{O})_{6-n}]^{2+}$	790	745	680	645	590	—
	( $n = 0$ )	( $n = 1$ )	( $n = 2$ )	( $n = 3$ )	( $n = 4$ )	—

\* Not calculated.

solution structure of the complex. The structural elucidation can be made by comparing the spectra of Fig. 3 with the published spectra of copper(II) complexes of ammonia.<sup>20</sup> To clarify the comparison,  $\lambda_{\text{max}}$  values for the complexes of this study together with those of the copper(II)–ammonia and  $-L^6$   $\{\text{L}^6 = N$ -[2-(dimethylamino)ethyl]ethanediamide $\}$  (ref. 13) systems are presented in Table 5.

Fig. 3 and Table 5 indicate the ML species for each of the four ligands investigated in the present study to have  $\lambda_{\text{max}}$  values between 650 and 690 nm. These approximate most closely to  $\lambda_{\text{max}} = 680$  nm for  $[\text{Cu}(\text{NH}_3)_2(\text{H}_2\text{O})_4]^{2+}$  suggesting that two nitrogen donor atoms are co-ordinated to the copper ion in each ML species with  $L = L^1$ – $L^4$ . Further support for this conclusion arises from the absence of M(HL) species in the potentiometric studies. In the pH range in which ML dominates (5–9) any unco-ordinated amino group would be protonated. The absence of M(HL), then, implies binding of at least two

nitrogens to each copper ion. Further, the relatively high stability of the ML species as shown in Tables 3 and 4 implies a denticity of at least two. Complexation through the amide nitrogens only, leaving the amino groups unbound, is highly improbable. It follows that likely structures for the ML species would be as sketched in Fig. 4(a) and 4(b). A third possibility is a structure in which only the two amine groups are bound to the copper ion. This structure has been proposed by Desseyn and co-workers<sup>22</sup> for the copper(II)– $L^3$  system in the solid state. We believe, however, that the size of the chelate ring argues against this structure. We favour structure (b), based on the following three arguments. First, co-ordination through a carbonyl group is feasible, as has been demonstrated in the copper(II)–glycinamide and  $-\beta$ -alaninamide systems.<sup>23</sup> With the latter two ligands, copper(II) ions form a chelate ring with the metal co-ordinated to both the amine and the carbonyl groups. Upon proton loss from the copper(II)–glycinamide complex, rearrange-

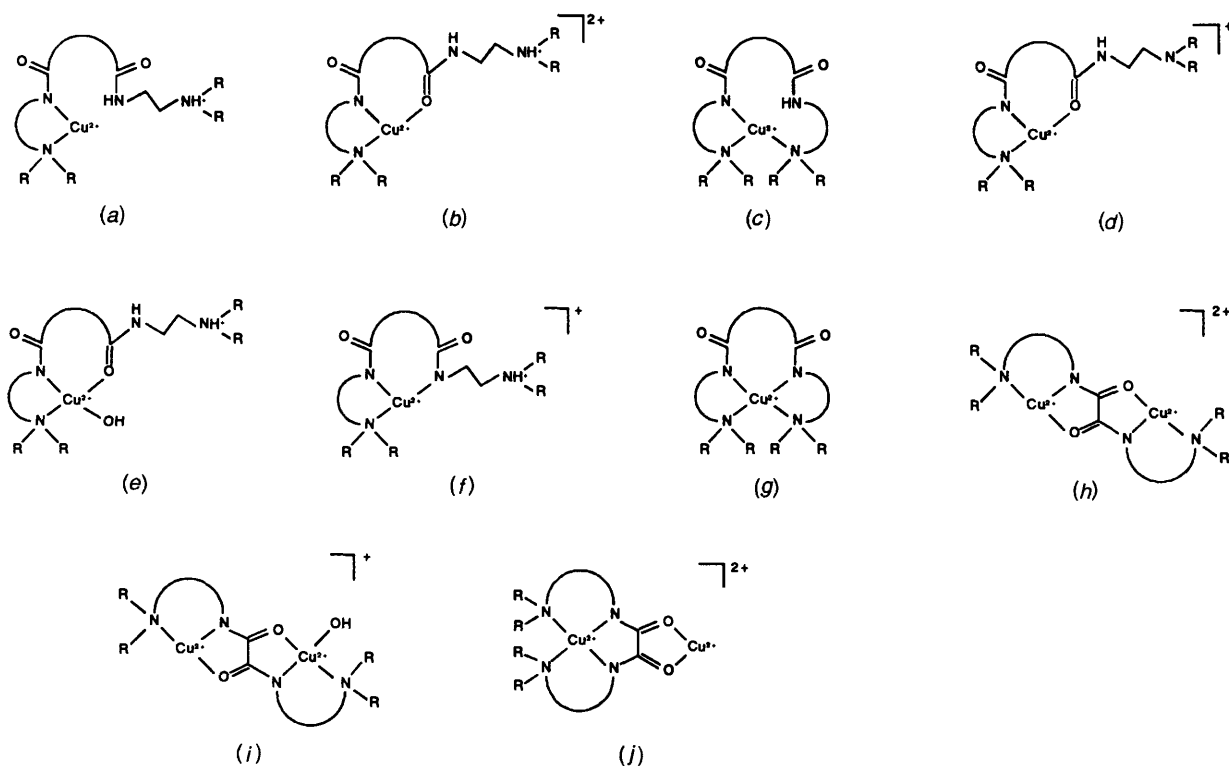


Fig. 4 Possible structures for different  $\text{Cu}_p\text{L}_q\text{H}_r$  complexes showing the site of metal-ion co-ordination and ligand protonation

ment of the chelate ring takes place such that co-ordination switches from the carbonyl to the amide nitrogen, yielding a structure similar to that in Fig. 4(a). The overall  $\log \beta_{11-1}$  for this complex is  $-1.44$ .<sup>23,24</sup> The corresponding copper(II)- $\text{L}^1$  complex has a  $\log \beta$  value of  $0.42$  (*i.e.*  $\log \beta_{110} - \log K_2$ ) which is some 2 logarithmic units greater than  $\log \beta_{11-1}$  for the copper(II)-glycinamide complex. This greater stability of the copper(II)- $\text{L}^1$  complex is consistent with structure (b) which has two chelate rings in contrast with the single chelate ring of the copper(II)-glycinamide complex. Co-ordination through one of the amines of the diamidodiamino ligands and the adjacent carbonyl oxygen is not expected as this would lead to the formation of less stable seven- and eight-membered rings which incorporate two  $\text{sp}^2$  centres. A second point favouring structure (b) over (a) is that Kaden and Zuberbühler<sup>25</sup> found a similar structure for the monosubstituted ligand *N*-[2-(dimethylamino)ethyl]ethanediamide ( $\text{L}^6$ ). Structure (b) is favoured further by the fact that although  $\text{L}^1$  and  $\text{L}^2$  have similar  $\log K$  values, the stabilities of the ML species differ by about 1.5 logarithmic units. If structure (a) were to apply those complexes would be expected to have similar stabilities.

The most likely structures for the  $\text{MLH}_{-1}$  species are given in Fig. 4(c)–4(f). As can be seen, these essentially differ according to the number of nitrogen atoms co-ordinated to the metal ion. Structure (c), suggested by Grieser and Fallab<sup>14</sup> for the ligand  $\text{L}^1$  with copper(II), seems unlikely due to the large size of the chelate ring. Of (c) and (d), both have only two nitrogen atoms in the co-ordination sphere of the copper(II) ion. The latter is improbable because, in the pH region in which the complex occurs, the unco-ordinated amine is likely to be protonated.

Structure (c) has been proposed by Zuberbühler and Kaden<sup>13</sup> for the ligand  $\text{L}^1$ . These authors based their argument on the similarity between the complexation of  $\text{L}^1$  and  $\text{L}^6$ . They also observed an absorption in the UV region of the latter species which was apparently due to hydroxo complexation and which was absent in the ML and  $\text{MLH}_{-2}$  species of  $\text{L}^1$ . A shift of only 20 nm between  $\lambda_{\text{max}}$  for ML and  $\text{MLH}_{-1}$  was determined for both  $\text{L}^6$  and  $\text{L}^1$  with copper(II). In contrast we observed a change in  $\lambda_{\text{max}}$  of 55 and 40 nm for the same species for the ligands  $\text{L}^1$  and  $\text{L}^4$  respectively

(Table 5). Secondly, the  $\lambda_{\text{max}}$  values of 620 and 630 nm respectively are lower than  $\lambda_{\text{max}}$  of  $[\text{Cu}(\text{NH}_3)_3(\text{H}_2\text{O})_3]^{2+}$  (645 nm). Furthermore the  $\lambda_{\text{max}}$  of the equivalent species  $\text{L}^6$ , on which Zuberbühler and Kaden based their argument, has a value of 690 nm, which is substantially different from those of the disubstituted ligands. Thus it seems probable that the  $\text{MLH}_{-1}$  species, particularly of  $\text{L}^1$  and  $\text{L}^4$ , has structure (f) in solution, although (e) cannot be ruled out completely.

The absorption maximum of 550–575 nm for the  $\text{MLH}_{-2}$  species of  $\text{L}^1$ ,  $\text{L}^2$  and  $\text{L}^4$  indicate the presence of four nitrogen atoms in the co-ordination sphere of the copper(II) ion.<sup>13</sup> Thus the most likely structure for this species is one with three contiguous chelate rings, (g). This structure is supported by several other studies<sup>18</sup> including the crystal structure of the four-co-ordinate nickel(II)- $\text{L}^3$  complex.<sup>21</sup> Co-ordination through the amide nitrogens involves loss of the amide protons resulting in the formation of a neutral species.

Ojima and Nonoyama<sup>18</sup> have proposed a structure for the  $\text{MLH}_{-3}$  complex of the copper(II)- $\text{L}^1$  system in which a hydroxyl ion displaces one of the amino groups from the co-ordination sphere of the metal ion. However, we believe this structure to be unlikely for the copper(II)- $\text{L}^3$  system considering the  $-30$  nm shift in  $\lambda_{\text{max}}$  in going from  $\text{MLH}_{-2}$  to  $\text{MLH}_{-3}$  (Table 5). Therefore a structure in which an axial water molecule of the  $\text{MLH}_{-2}$  complex has been replaced by an hydroxyl ion is proposed.

The  $\lambda_{\text{max}}$  values of the  $\text{M}_2\text{LH}_{-2}$  and  $\text{M}_2\text{LH}_{-3}$  species of the copper(II)- $\text{L}^1$  system are again virtually the same as that of the ML species, indicating the co-ordination of two nitrogen atoms per metal ion. Furthermore, only one absorption maximum is observed in the electronic spectra of these species, indicating a similar environment for both the copper(II) ions. For these data structures (h) and (i) are proposed for species  $\text{M}_2\text{LH}_{-2}$  and  $\text{M}_2\text{LH}_{-3}$  respectively. Further evidence supporting these structures is given by the crystal structure of the  $[\text{Cu}_2\text{L}^1(\text{NCS})_2(\text{dmf})_2]^{2+}$  (*dmf* = dimethylformamide) complex.<sup>26</sup>

In the case of the copper(II)- $\text{L}^3$  system an additional structure may be suggested for the  $\text{M}_2\text{LH}_{-2}$  species. The UV/VIS spectrum of this species has a shoulder at  $\approx 700$  nm and a  $\lambda_{\text{max}}$  of 600 nm (Fig. 3). This suggests that the two

copper(II) ions in the complex have different electronic environments. A structure which is consistent with these results is shown in Fig. 4(j). Structures of this type have been found in mixed complexes with bis(2,2'-bipyridine)nickel(II),<sup>27</sup> bis(2,2'-bipyridine)copper(II) and (N,N,N',N'',N'''-pentaethyldiethylenetriamine)copper(II).<sup>28</sup> The initial complexation of the four nitrogen atoms fixes the carbonyl oxygens in a favourable position for further co-ordination to another metal ion. However, structure (h) has been found in the crystal structure of [Cu<sub>2</sub>L<sup>3</sup>(NO<sub>3</sub>)<sub>2</sub>].<sup>22</sup>

### Acknowledgements

The authors thank the Foundation for Research Development and the University of Cape Town for financial assistance. The University's Information Technology Services is thanked for the smooth running of the programs.

### References

- 1 G. E. Jackson and M. J. Kelly, *Inorg. Chim. Acta*, 1988, **152**, 215; *J. Chem. Soc., Dalton Trans.*, 1989, 2429; Part 4, G. E. Jackson and B. S. Nakani, *J. Chem. Soc., Dalton Trans.*, 1996, 1373.
- 2 P. M. May, P. W. Linder and D. R. Williams, *J. Chem. Soc., Dalton Trans.*, 1977, 588.
- 3 G. E. Jackson, M. J. Byrne, G. Blekkenhorst and A. J. Hendry, *Nucl. Med. Biol.*, 1991, **18**, 855.
- 4 *Complexometric Assay Methods with Titriplex*, 3rd edn., E. Merck, Darmstadt.
- 5 J. Bassett, R. C. Denney, G. H. Jeffery and J. Mendham, *Vogel's Textbook of Quantitative Inorganic Analysis*, 4th edn., Longman, London, 1978.
- 6 K. V. V. Voyi, Ph.D. Thesis, University of Cape Town, 1988.
- 7 P. M. May, D. R. Williams, P. W. Linder and R. G. Torrington, *Talanta*, 1982, **29**, 249.
- 8 P. M. May, K. Murray and D. R. Williams, *Talanta*, 1985, **32**, 483; 1988, **35**, 825.
- 9 A. Albert and D. Serjent, *Ionization Constants of Acids and Bases*, Methuen, London, 1962, p. 20.
- 10 A. Sabatini, A. Vacca and P. Gans, *Talanta*, 1974, **21**, 53.
- 11 D. Dyrssen and I. Hanson, *Mar. Chem.*, 1972, **1**, 37.
- 12 E. Högfeldt, *Stability Constants of Metal-ion Complexes, Part A: Inorganic Ligands*, IUPAC, Pergamon, Oxford, 1982.
- 13 A. Zuberbühler and Th. Kaden, *Helv. Chim. Acta*, 1968, **51**, 1805.
- 14 R. Grieser and S. Fallab, *Chimia*, 1968, **22**, 90.
- 15 S. Cattoir, personal communication.
- 16 K. F. Purcell and J. C. Kotz, *Inorganic Chemistry*, W. B. Saunders Company, London, 1977.
- 17 U. Kramer-Schnabel and P. W. Linder, *Inorg. Chem.*, 1991, **30**, 1248.
- 18 H. Ojima and K. Nonoyama, *Coord. Chem. Rev.*, 1988, **921**, 857.
- 19 M. Kodama, T. Yatsunami and E. Kimura, *J. Chem. Soc., Dalton Trans.*, 1979, 1783.
- 20 H. H. Jaffé and M. Orchin, *Theory and Applications of Ultraviolet Spectroscopy*, Wiley, New York, 1962.
- 21 R. M. Lewis, G. H. Nancollas and P. Coppens, *Inorg. Chem.*, 1972, **11**, 1371.
- 22 F. J. Quaeqhaegens, H. O. Desseyne, S. P. Perlepes, J. C. Plakatouras, B. Bracke and A. T. H. Lenstra, *Transition Met. Chem.*, 1991, **16**, 92.
- 23 R. M. Smith and A. E. Martell, *Critical Stability Constants, Vol. 2: Amines*, Plenum, New York, 1975.
- 24 O. Yamauchi, H. Miyata and A. Nakahara, *Bull. Chem. Soc. Jpn.*, 1971, **44**, 2716.
- 25 Th. Kaden and A. Zuberbühler, *Helv. Chim. Acta*, 1968, **51**, 1797.
- 26 A. Yoshino and W. Nowacki, *Z. Kristallogr.*, 1974, **139**, 337.
- 27 H. Ojima and K. Nonoyama, *Z. Anorg. Allg. Chem.*, 1977, **429**, 282.
- 28 Y. Journaux, J. Sletten and O. Khan, *Inorg. Chem.*, 1985, **24**, 4063.

Received 3rd April 1996; Paper 6/02340A